A MICRO-REVIEW ON PROSPECTS AND CHALLENGES OF PEROVSKITE MATERIALS IN ORGANIC-INORGANIC HYBRID SOLAR CELL APPLICATIONS

M. SALIM[a], MD. SHAHADAT HUSSAIN CHOWDHURY[a], M. S. HOSSAIN[b], M. A. ISLAM[b, c*]

[a]*Department of Chemistry, School of Physical Sciences, Shahjalal University of Science & Technology, Sylhet, Bangladesh*
[b]*Solar Energy Research Institute, National University of Malaysia, 43600 Bangi, Selangor, Malaysia*
[c]*Graduate School of Material Science, Nara Institute of Science and Technology, Ikoma, Nara 630-0101, Japan*

Last few years, the perovskite materials have attracted great attention in organic-inorganic solar cells due to their excellent light-harvesting properties, tune-able direct band gap, high molar extinction coefficient, high carrier mobility. This platform makes new opportunities for the development of solution-processed, high-efficiency and low-cost solar cells. The power conversion efficiency of perovskite based organic-inorganic hybrid solar cells has now above 15%, making it competitive with crystalline Si solar cells. This review summarised the current performance and drawback of perovskite materials in solar cell applications. Also the versatile synthesizes methods of perovskite thin film has been discussed in this article.

1. Introduction

The demand of energy is increasing followed by the increase of world population. Therefore, the development of clean alternatives to existing conventional power generation methods from coal and fossil fuel is immensely important to preserving the global environment and assuring sustainable economic growth [1]. Photovoltaic (PV) technology seems one of the most effective ways to reduce the energy crisis. Silicon technology (first generation solar cell) is the pioneer for PV solar cells last 20 years. Crystalline silicon solar cell [2] shows high power conversion efficiency (PCE) of more than 20%. However, this Si PV technology is facing a strong challenge due to relatively high production cost at large scale. The second-generation solar cell (thin-film) such as cadmium telluride (CdTe), cadmium sulphide (CdS), cadmium selenide (CdSe), lead sulphide, lead selenide (PbSe) and copper indium gallium selenide (CIGS) seems to be the low cost than first generation Si solar cells and they exhibit PCE of around 19.6% for 1 cm^2 [2-11]. But, unfortunately, they are still facing problems in large-scale production. However, third-generation multi-layer tandem solar cell made of amorphous silicon and gallium arsenide are prospective due to low cost and higher efficiency. But, complex fabrication process is a big issue for them. On the other hand, dye-sensitized solar cell (DSCs) is also a highly promising solar technology due to their simple fabrication process, efficient, versatile and low cost. The dye-sensitized solar cell (DSC) invented in 1991 by using mesoporous titania film for sensitization and liquid electrolyte for photon absorption [12, 13]. The mesoporous titania film enhances the surface

---

* Corresponding author: aminbgm@yahoo.com

area by 1000 times compared to flat surface which increase the potential photon absorption and 12.3% photoelectric conversion efficiency has been achieved [13]. However, the liquid electrolyte is the main drawback of the DSC design which is not stable to temperature. The electrolyte can freeze at low temperatures ending power production and potentially leading to physical damage. Another problem is the use of costly ruthenium (dye), platinum (catalyst) and conducting glass or plastic (contact) in DSCs. A third major drawback is that the electrolyte solution contains volatile organic solvents which are hazardous to human health and the environment. A solid electrolyte instead of the liquid electrolyte has been a main ongoing field of research in DSCs. Currently solidified melted salts have shown some promises, but suffer from higher degradation during continued operation, and are not flexible [14-28].

Currently, methylammonium lead halide ($CH_3NH_3PbX_3$, X = halogen; CH_3NH_3: MA) and its mixed-halide perovskite crystal structures, have been introduced as light harvesters in solar cells [27- 29]. The advantages of these compounds have already been shown as an important example due to their potentially useful physical properties such as nonlinear optical properties, electroluminescence, organic-like mobility, magnetic properties, and conductivity [30-33]. The band gap of these materials can be tuned easily by chemical management to form an array of translucent colors, and this feature can be utilized to make colourful solar designs. More importantly, they are exhibiting ambipolar transport, allowing them to replace the hole or electron transporter in hybrid solar cells [28, 34-35]. They can also be synthesized by simple solution-process and cheap techniques.[28, 33, 36] Therefore; these materials are highly potential as an ideal light absorber for low-cost and high efficiency solar cells [26-27, 29, 37]. Recently, Burschka and co-workers reported 15% efficiency solar cell with $CH_3NH_3PbBr_3$ target efficiency of 20% identified as a feasible goal [38].

2. Structure of perovskite materials

The first perovskite type material was discovered in the Ural Mountains of Russia by Gustav Rose (1839). It was later named after a Russian mineralogist L.A. Perovski, who first characterized the structure. The crystal structure of a $CaTiO_3$ type orthorhombic perovskite was first published in 1945 by Helen Dick McGaw [39]. Research on perovskites did not catch on until the mid-40s, when there was a dramatic increase in solid-state research, especially focusing on ferroelectric materials like perovskites. Since the 1940s, perovskite materials have been a hot topic of research, and will remain a promising research frontier far into the future.

The general chemical formula for perovskite compounds is ABX_3, where 'A' and 'B' are two cations of very different sizes, and X is an anion that bonds to both (Fig. 1(left)). The 'A' atoms are larger than the 'B' atoms. The ideal cubic-symmetry structure has the B cation in 6-fold coordination, surrounded by an octahedron of anions and the 'A' cation in 12-fold cub-octahedral coordination. The relative ion size requirements for stability of the cubic structure are quite stringent. Therefore, slight buckling and distortion can produce several lower-symmetry distorted versions, in which the coordination numbers of 'A' cation, 'B' cation or both are reduced [40].

The formation ability of perovskite structure is based on its geometric tolerance factor (t) [41],

$$t = (rA + rX)/[H_2(rB + rX)] \qquad (1)$$

where, rA, rB and rX are the effective ionic radii for A, B and X ions, respectively.

An ideal cubic perovskite is estimated when t = 1 while octahedral distortion is estimated when t < 1 [42]. If, t < 1, symmetry of perovskite decreases, and affects the electronic properties of the material [42]. Li et al reported that the formability is expected for 0.813 < t < 1.107 for alkali metal halide perovskite [43]. Shannon was calculated the rA in $APbX_3$ (X = Cl, Br, I) perovskite for t = 0.8 and t = 1 based on effective ionic radii [44] and found that to form a perovskite structure, a cations with radii between ~1.60 A° and ~2.50 A° is required. Thus, methylammonium cation is

suitable for lead halide perovskite because its ionic radius is 1.8 A°. Since the tolerance factor of $CH_3NH_3PbI_3$ was calculated ≤ 1.0, deviation from an ideal cubic structure is anticipated. Fig. 1(right) shows the X-ray diffraction pattern of powder $CH_3NH_3PbI_3$ formed from reaction between CH_3NH_3I and PbI_2. The peaks were indexed as a tetragonal phase with lattice parameters of a = b = 8.883 A° and c = 12.677 A° [45].
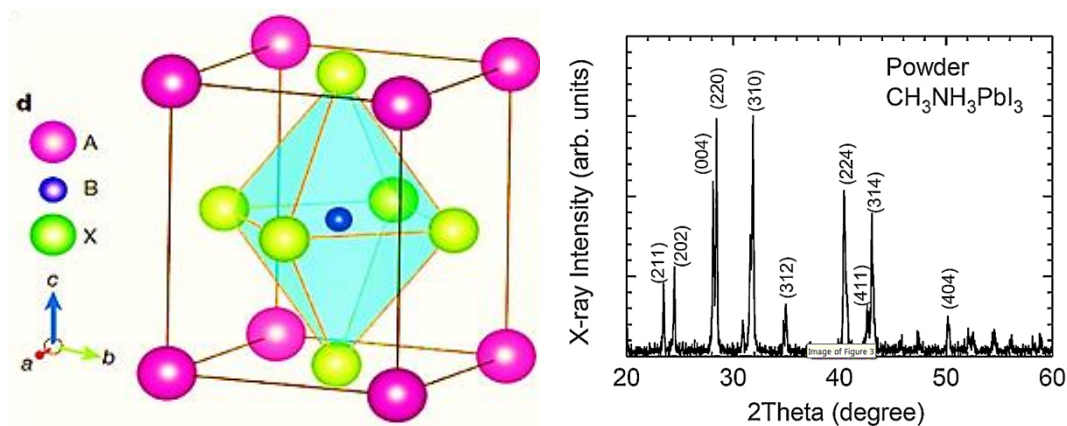
Fig. 1(left) Crystal structure of the perovskite materials, (right) X-ray diffraction patterns for CH₃NH₃PbI₃ powder, which was prepared by reaction of CH₃NH₃I with PbI₂ in gamma-butyrolactone solution [45]

Perovskites are found naturally as kimberlites, carbonatites, and calcareous skarns ($CaTiO_3$). More specifically, some examples of materials with perovskite structure include: $CaTiO_3$, $MgSiO_3$, $SrFeO_3$, $BaTiO_3$, $SrZrO_3$, and the non-oxide $KMgF_3$. These materials are commonly found in the Ural Mountains in Russia, Magnet Cove in the US, Mt. Vesuvius, Sweden, Germany and deep within the earth. Perovskites are stable at an extremely wide range of conditions and have unique chemical and physical properties, which make them an ideal material for many technological applications [45].

3. Current performances of perovskite materials as light harvester

Although the first efficient organic-inorganic perovskite solar cells were reported only in mid-2012, extremely rapid progress was observed during 2013 with energy conversion efficiency of 16.2% at the end of the year [46]. Till today, iodide perovskite (CH3NH3PbI3) and bromine perovskite ($CH_3NH_3PbBr_3$) are found as the most important light harvesting materials in perovskite solar cells due to their high extinction coefficient and very good incident-photon-to-current conversion efficiency (IPCE). The bandgap of $CH_3NH_3PbI_3$ is 1.55 eV which is close to the optimum bandgap (1.5 eV) for PV performance. The $CH_3NH_3PbI_3$ material has good extinction coefficient with excellent external quantum efficiency until 800 nm of wave length (absorbed around 80% in the 400-600 nm range). This material show a significant impact on harvesting photons in the visible range of the solar spectra and part of the near-infrared (Fig. 2) [47, 48]. Therefore, the PCE of the material increased from 3.8% [29] to 15.7% [49] within a short time. Nevertheless, the drawback is the achieved current density (Jsc = 17 mAcm^{-2}) which is very low as compared to its theoretical current density (Jsc = 27 mAcm^{-2}). Another form of iodide perovskite is midinium lead triiodide (FAPbI3) show a broader band gap as 1.84 eV compared to CH3NH3PbI3. It has ability to absorb till 840 nm light which has a significant effect on performance of solar cells. Eperson [50] utilized FAPbI3 in perovskite solar cells and achieved 14.2% PCE. However, the average value of Voc (0.85 V) and FF (60%) was reduced compared to $CH_3NH_3PbI_3$, the average Jsc was raised to 18.8 mAcm^{-2} and a record Jsc value of 23.3 mAcm^{-2} was also reported again later [50]. As seen the above reports, it has been found that the achieved

1292

Jsc and FF till today is lower than theoretical value. Thus there should be much more rooms to improve the efficiency of the perovskite solar cells.
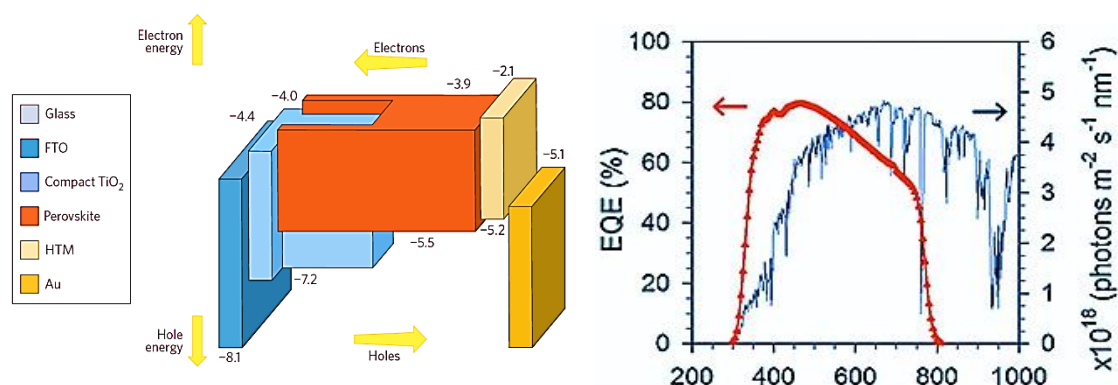
Fig. 2 (left) Band structure for a perovskite solar cell with structure
glass/FTO/TiO₂/perovskite/HTM/Au, (right) External quantum efficiency measured
for CH₃NH₃PbI₃perovskite solar cell under the 1.5 AM solar spectra [51]

Etgar et al. reported $CH_3NH_3PbI_3$ as both light absorber and hole transport material in $CH_3NH3PbI_3$/TiO_2 heterojunction solar cell by using a 300 nm thick $CH_3NH_3PbI_3$ film as shown in Fig. 3 [35]. This heterojunction solar cell attained a remarkable PV performance. For 1 sun illumination, they reported PCE of 8% with short-circuit photocurrent (Jsc) of 18.8 mAcm^{-2}, open-circuit voltage (Voc) of 0.71 V, and fill factor (FF) of 0.60. The solar cell efficiency was observed to decrease with the increase of light intensity. They found PCE of 7.3% at 10 sun intensity with Jsc of 2.1 mAcm^{-2}, FF of 0.62, and Voc of 0.57 V and PCE of 5.5% at 100 sun intensity with Jsc of 16.1 mAcm^{-2}, FF of 0.57, and Voc of 0.63 V.This heterojunction solar cell depicted a depletion layer due to the charge transfer from the electron accepting contact to the $CH_3NH_3PbI_3$ layer. The $CH_3NH_3PbI_3$ perovskite harvested the light on light illumination, and consequently electrons were transferred from the $CH_3NH_3PbI_3$ perovskite to the TiO_2 and holes were transported to the gold contact (Fig. 3).

A depletion region which extended to both n and p sides was measured by Mott-Scottky analysis. The charge separation was assisted by the build-in field of the depletion layer and reduces the back reaction of the electrons from the TiO_2 film to the $CH_3NH_3PbI_3$ film. The iodide material undergoes a phase transition from tetragonal to cubic when it is heated above 55-60 °C. As a result, a narrow bandgap is formed [52].
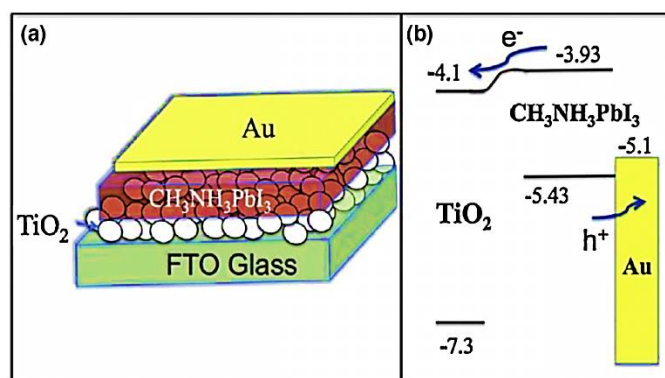
Fig. 3 (a) Device configuration of CH₃NH₃PbI₃/TiO₂ heterojunction solar cell
and (b) charge separation process [48]

Lee et al. reported that Cl and I mixed halide perovskite material ($CH_3NH_3PbI_2Cl$) could be possible to use as both light harvester and electron transporter [28]. The above

material showed superior light absorbing abilities to the visible and near infrared spectrum than $CH_3NH_3PbI_3$. The efficiency of 10.9% with Voc =1.10V was achieved by using this mixed halide perovskite material in hybrid organic/inorganic solar cells of structure FTO/bl-TiO_2/Al_2O_3-$CH_3NH_3PbI_2Cl$/spiro-OMeTAD. The spiro-OMeTAD in this bulk heterojunction collects the holes and transports them to the back contact. The mesoporous Al_2O_3 acts as a scaffold in a small nanometer thin layer of $CH_3NH_3PbI_2Cl$ carrying electronic charges out of the device through FTO photo-anode. The mesoporous Al_2O_3 as an inert scaffold can also transport the electron to the anode due to the large diffusions length of the perovskite material. Nevertheless, Koutselas et al. used TiO_2 instead of Al_2O_3 in the above structure [30]. They reported the PCE of about 8% for TiO_2/ $CH_3NH_3PbI_2Cl$ /spiro-OMeTAD/Ag solar cell under full sun illumination.
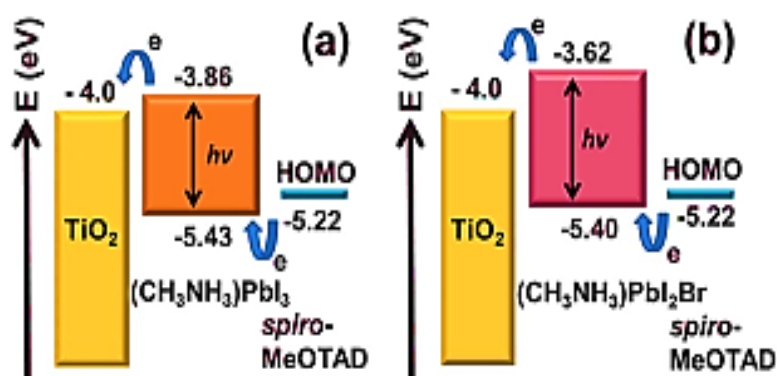
Fig. 4 Schematic energy level diagrams of the TiO_2 NWAs, organometallic perovskite sensitizers – (a) $CH_3NH_3PbI_3$ and (b) $CH_3NH_3PbI_2Br$ [52]

Qiu et al. reported a solution processed all-solid state hybrid solar cell based on above mixed halide perovskite sensitizer, $CH_3NH_3PbI_2Br$ and 1D TiO_2 nanowire arrays (NWA) with a PCE of about 5% [53]. They sketch the band alignment scheme for the hybrid photovoltaic cells (Fig. 4). It is clearly seen that the higher conduction band edges of $CH_3NH_3PbI_2Br$ bring out a larger driving force for the photogenerated electrons to transfer from the sensitizer to the TiO_2 NWAs. This could be lead to enhanced photogenerated electron injection efficiency from the $CH_3NH_3PbI_2Br$ sensitizer to the TiO2 nanowire arrays [54, 55] compared to the $CH_3NH_3PbI_3$-based device [53].
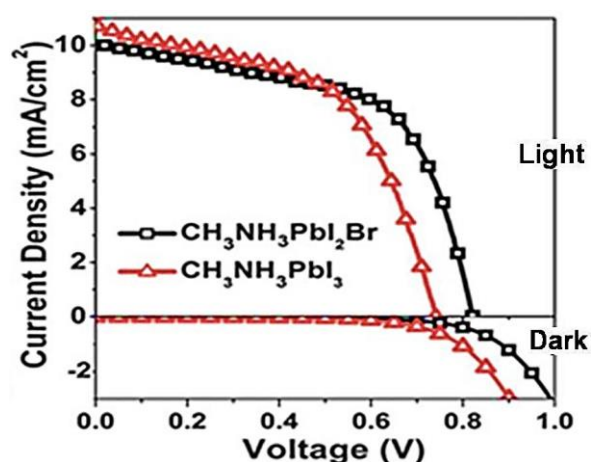
Fig. 5 Current density–voltage (J–V) characteristics of the TiO_2 NWAs/perovskite sensitizer/spiro-MeOTAD hybrid solar cells under 100 mW cm^{-2} AM 1.5 illumination and in the dark [55]

Fig. 5 shows the J-V charactersistics curves of mixed halide perovskite $CH_3NH_3PbI_2Br$ and halide perovskite $CH_3NH_3PbI_3$ reported by Robel et al. [55]. It is observed that the cell open circuit voltage is significantly increased for $CH_3NH_3PbI_2Br$ solar cells. However, there is a smaller dark current was observed on the photovoltaic cell based on $CH_3NH_3PbI_2Br$ compared to that of the $CH_3NH_3PbI_3$-based device. This means that the solar cell featuring the TiO_2 NWAs/ CH3NH3PbI2Br sensitizer/spiro-MeOTAD/Au junction can better restrain the recombination of the photogenerated electrons injected into the TiO_2 NWAs and the hole extracted into spiro-MeOTAD [53]

Table 1 shows the progress in perovskite solar cell efficiency by year. Since 2009, Kojima et al. have been used organolead halide perovskites for solar cells. At that time, liquid perovskite light absorbers were used as sensitizers in dye-sensitized solar cells (DSSC). The life time or stability of perovskite DSSC was very short. In 2012, a long-term stable perovskite solar cell was designed by replacing liquid with solid HTM. Since then, solid-state perovskite-containing solar cells have been called perovskite solar cells. In 2014, the Korean Research Institute of Chemical Technology (KRICT) reported record PCE of 17.9%, which was certified by the National Renewable Energy Laboratory (NREL) [64].

Table 1 Summary of the reported perovskite solar cells performance parameters according to the type of light harvesting materials and years

Author/ Year	Location	Light harvester/HTM/ETM	Jsc [mAcm^{-2}]	Voc [V]	FF	PCE [%]	Ref.
Kojima et al., 2009	Japan	$CH_3NH_3PbI_3$	11	0.61	0.57	3.81	[29]
Kojima et al., 2009	Japan	$CH_3NH_3PbBr_3$	5.58	0.97	0.6	3.14	[29]
NOH et al., 2013	Korea	$CH_3NH_3PbI_3$	18.3	0.87	0.66	10.4	[56]
Eperon, 2014	UK	$CH_3NH_3PbI_{3-x}Cl_x$	20.3	0.89	0.64	11.4	[57]
Edri et al., 2013	Israel	$CH_3NH_3PbBr_3$ & ETM	1.57	1.06	0.43	0.72	[58]
Qiu et al., 2013	China	$CH_3NH_3PbI_2Br$	10.12	0.82	0.59	4.87	[53]
Qiu et al., 2013	China	$CH_3NH_3PbI_3$	10.68	0.75	0.55	4.3	[53]
Liu et al., 2013	UK	$CH_3NH_3PbI_{3-x}Cl_x$ & ETM	21.5	1.07	0.68	15.4	[59]
Laban et al., 2013	Israel	CH3NH3PbI3 & HTM	18.8	0.71	0.6	8	[48]
Kumar et al, 2013	Singapore	$CH_3NH_3PbI_3$	11.27	1.08	0.45	5.54	[60]
Kumar et al, 2013	Singapore	$CH_3NH_3PbI_3$	16.98	1.02	0.51	8.9	[60]
Kumar et al, 2013	Singapore	$CH_3NH_3PbI_3$	5.57	0.99	0.4	2.18	[60]
Kumar et al, 2013	Singapore	$CH_3NH_3PbI_3$	7.52	0.8	0.43	2.62	[60]
Etgar et al., 2012	Israel	$CH_3NH_3PbI_3$ & HTM	16.1	0.63	0.57	5.5	[35]
Kim et al., 2013	Singapore	$CH_3NH_3PbI_3$	15.5	0.96	0.63	9.4	[47]
Moon et	Switzerland	$CH_3NH_3PbI_3$ & ETM	17.3	1.07	0.59	10.8	[61]

Author/ Year	Location	Light harvester/HTM/ETM	Jsc [mAcm^{-2}]	Voc [V]	FF	PCE [%]	Ref.
al., 2013							
Ball et al., 2013	UK	$CH_3NH_3PbI_{1-x}Br_x$ & ETM	18	1.02	0.67	12.3	[37]
Heo et al., 2013	Korea	$CH_3NH_3PbI_3$	16.4	0.9	0.61	9	[62]
Heo et al., 2014	Korea	$CH_3NH_3PbI_3$	16.5	0.99	0.997	12	[62]
Niu et al., 2014	China	$CH_3NH_3PbI_3$	13.66	0.71	0.48	4.69	[63]
Niu et al., 2015	China	$CH_3NH_3PbI_3$	11.11	0.86	0.46	4.6	[63]

4. Drawbacks of perovskite materials in solar cells applications

Strong optical absorption is the key to the outstanding performance of the perovskite solar cells, reducing both the required thickness and the challenges in collecting photogenerated carriers. Fig. 6 shows the absorption measurements curves of perovskite materials compared to other solar cell materials. It is clearly seen that perovskite materials has higher absorption co-efficient compared to other materials. However, perovskites solar cells have advantages of easy and low processing costs, high conversion efficiencies, possible to fabricate as flexible or partially transparent modules make them unique and attractive solar cell than others. But, one big challenge for perovskite solar cells is the aspect of long-term stability. The perovskite films are seriously sensitive to moisture in air because of the hygroscopic amine salts make devices highly prone to rapid degradation in moist environments [65].
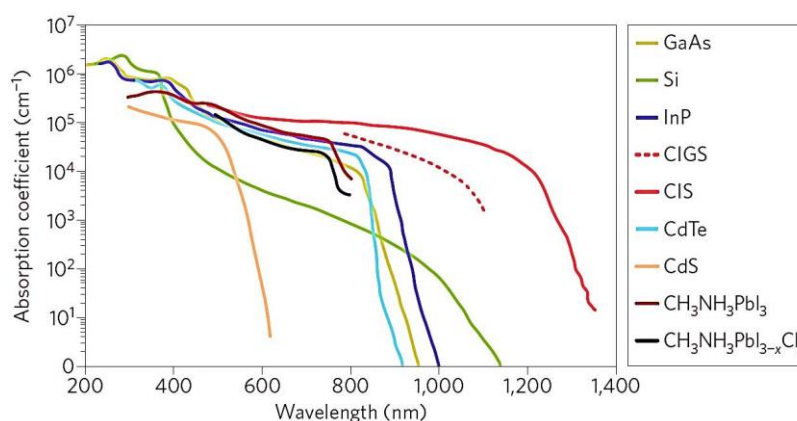
Fig. 6 Absorption coefficient of CH3NH3PbI3 [66] and $CH_3NH_3PBI_{3-x}Cl_x$ [67] compared to other solar cell materials (various sources)

In particular, $CH_3NH_3PbI_3$ is more sensitive to air than $CH_3NH_3PbBr_3$ [33]. The PCE of the encapsulated $MAPb(I_{1-x}Br_x)_3$ (x = 0, 0.06, 0.20, 0.29) has been measured to examine the stability of $MAPb(I_{1-x}Br_x)_3$ under ambient conditions with controlled humidity along with the storage time, as shown in Fig. 6 [26]. The PCE of $CH_3NH_3PbI_3$ solar cells did not degrade significantly at low humidity (<50%). However, degradation has been occurred at relatively high humidity (≥55%) showing a colour change from dark brown to yellow. Therefore, the solar cells were intentionally exposed to relatively high humidity (55%) for one day while the other days it was kept at 35% humide condition. Surprisingly, serious degradation of PCE has been shown for $MAPb(I_{1-x}Br_x)_3$ (x = 0, 0.06) after exposure

to 55% humidity while $MAPb(I_{1-x}Br_x)_3$ (x = 0.2, 0.29) maintained the PCE. A low sensitivity for $MAPb(I_{1-x}Br_x)_3$ (x ≥ 0.2) to humidity might be associated with its compact and stable structure. Because the substitution of bigger iodine atoms with smaller bromine atoms in $MAPb(I_{1-x}Br_x)_3$ leads to the reduction of the lattice constant and a transition to the cubic phase [26].

Grätzel et al. demonstrated that the device fabrication should be carried out under controlled atmospheric conditions and with a humidity of <1% [63]. Niu and co-workers also found a similar phenomenon that perovskite films tend to degrade in a high humidity environment. They also presented the degradation reactions as follows:

$$CH_3NH_3PbI_3(s) \underset{\longleftarrow}{\overset{H_2O}{\longrightarrow}} CH_3NH_3I(aq) + PbI_2 (s)$$
$$CH_3NH_3I (aq) \underset{\longleftarrow}{\longrightarrow} CH_3NH_2(aq) + HI(aq)$$
$$4HI (aq) + O_2 (g) \underset{\longleftarrow}{\longrightarrow} 2H_2O (g) + 2I_2 (s)$$
$$2HI (aq) + h\nu \underset{\longleftarrow}{\longrightarrow} H_2(g) + I_2(s)$$
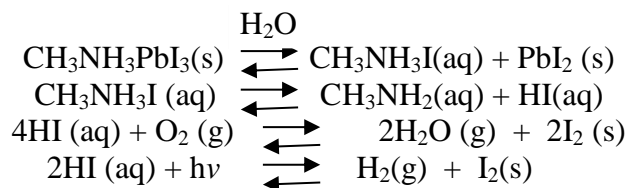
To prevent the corrosion from moisture they proposed that the $CH_3NH_3PbI_3$ films should be post-modified by Al_2O_3. After modification the films were well protected and the absorption of the film decreases less than without modification. The main function of the Al_2O_3 layer is to separate the $CH_3NH_3PbI_3$ films from the air physically. As a result, the Al_2O_3 layer protects $CH_3NH_3PbI_3$ films from degradation. The efficiency of the solar cells with and without post-modification by Al_2O_3 is 4.60% and 4.69% respectively as shown in Fig. 8. When the film was exposed to air for more than 18 hours with humidity of 60% at 35 °C under sunlight, the device without modification has been shown only 0.942% PCE, which is only 20% of the original PCE without degradation and with post-modification has been shown 2.23%, which is 48% of the original PCE without degradation [63].
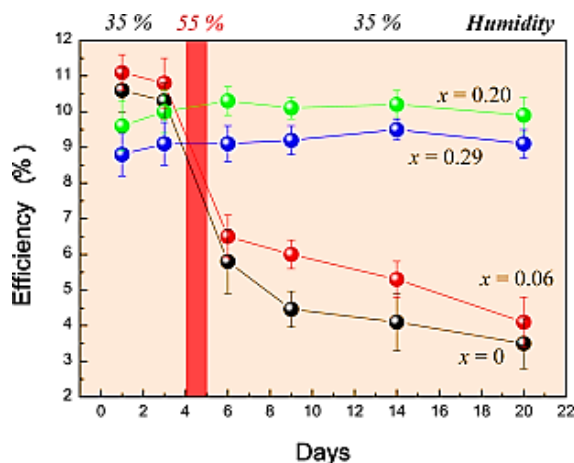
Fig. 7 PCE variation of the heterojunction solar cells based on MAPb $(I_{1-x}Br_x)_3$ (x = 0, 0.06, 0.20, 0.29) with time stored in air at room temperature without encapsulation. The humidity was maintained at 35%, and the cells were exposed to a humidity of 55% for one day on the fourth day to investigate performance variation at high humidity [26]

Another drawback for all-solid-state perovskite solar cells is the recombination of electrons. Perovskite materials could hardly cover the surface of the TiO_2 photoanode completely [36, 47]. Similar findings are also reported by Niu and co-workers [63]. The uncovered sites on TiO2 particles could be in contact with HTMs, resulting in electron recombination from the conduction band (CB) of TiO_2 to HTMs. The recombination resistance could be increased from 187.0 ohm to 424.9 ohm by post-modification with

Al_2O_3. The increased interface resistance retard back reaction from the TiO_2 CB to spiro-OMeTAD. The hole cover of Al_2O_3 on TiO_2 and $CH_3NH_3PbI_3$ is the reason for the retard back reaction. Following the above way, the direct contact between TiO_2 and spiro-OMeTAD is successfully avoided. The wide-band of TiO_2 could protect electrons in TiO_2 from recombination with spiro-OMeTAD which is shown in Fig. 9 [63].
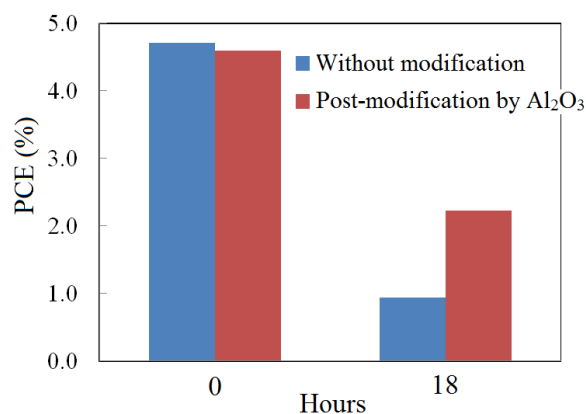
Fig. 8 Degradation of efficiency versus time exposed to air with a humidity of 60% at 35 °C under sunlight [63]
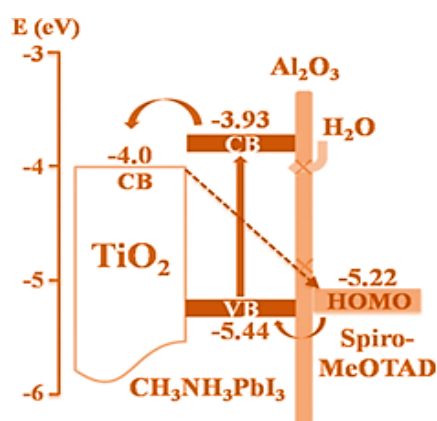
Fig. 9 Energy level diagrams of the device with post modification by Al_2O_3 [63]

Additionally, the toxicity of lead is still a problem in hybrid organic-inorganic lead halide perovskite solar cells. The tin (Sn) and Zinc (Zn) could be one of the suitable candidates for this. However, it easily oxidized to make Sn^{4+} that creates metal like behaves in semiconductor which lowers the PV performance [68].

5. Current synthesis procedures of perovskite materials

There are many factors to improve the efficiency as well as the stability of the organic-inorganic perovskite solar cells; the synthesis process is one of the key factors among them. Mainly four methods are commonly used for the synthesis of perovskite materials so far namely chemical method (or one-step precursor deposition method), dual-source evaporation method, sequential deposition method, and vapour-assisted solution method.

5.1 Chemical Method

This method is the most popular thin film deposition for the perovskite hybride solar cells due to its simplicity. Generally, the powder of RAX (R= alkyl, A= NH$_3$, X= I, Br) and PbX$_2$ (X= I, Br, Cl) is mixed at the 1:1 (stoichiometry) or 3:1 (non-stoichiometry) mole ratio in high boiling point aprotic polar solvents like DMF, DMAc, DMSO, NMP, GBL, etc. at elevated temperature for several hours to get a clear solution of perovskite materials. Mentioned that RAX was synthesized by reacting of 40% methylamine in methanol solution with HX followed by recrystallization. Then the perovskite precursor solution is utilized for the in situ formation of organometal halide perovskite by spin coating on the TiO2 surface [29, 69]. So far this method has been achieved the highest record PCE of 15.9% [70].

5.2 Dual-Source Evaporation Method

This method for the preparation of perovskite thin film was first developed by Salau [71] and then by Mitzi and co-workers [72]. Liu and co-workers [59] modified the deposition condition to make the thin film of mixed halide perovskite as the harvesting layer in a planar heterojunction solar cell. The perovskite absorber was deposited by a dual-source evaporation system (Fig. 10) (Kurt J. Lesker Mini Spectros) with ceramic crucibles (organic light-emitting diode sources) in a nitrogen-filled glove box.
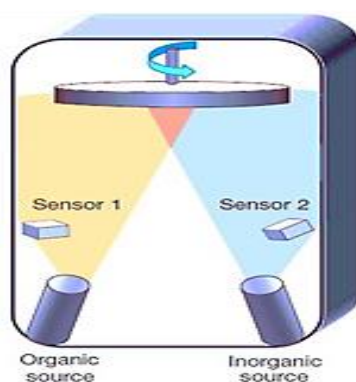
Fig. 10 Dual-source thermal evaporation system for perovskite compound [59]

In this process, methylammonium iodide (CH$_3$NH$_3$I) and lead chloride (PbCl$_2$) were evaporated simultaneously from separate sources at 10^{-5} mbar with 4:1 molar ratio, based on the reading of the sensors above the crucibles. After evaporation, a dark reddish-brown colour was observed immediately. Then the perovskite absorbers are annealed and hole-transporter layer is deposited on top of it by spin-coating process. The vapour-deposited perovskite devices were made on FTO-coated glass. A compact layer of TiO$_2$ was deposited on the FTO-coated glass by spin-coating (solution-processing) with a mildly acidic solution of titanium isopropoxide in ethyl alcohol, and consequently the perovskite absorber was deposited on the compact TiO$_2$-coated FTO substrate. It was found that the absorber layer was extremely uniform with crystalline platelets at the nanometer scale while the solution processed film only partially covered the substrate containing voids between micrometer-sized crystalline platelets which extend directly to the compact TiO$_2$-coated FTO glass. Due to the superior uniformity of the coated absorber layer 15.4% efficiency was observed [37, 59].

5.3 Sequential Deposition Method

The sequential deposition method was first developed by Mitzi and co-workers [73, 74]. In a sequential deposition method, MI$_2$ (M = Pb, Sn) film and organic salt solution were prepared separately. Then the perovskite was fabricated by dipping process.

At first, the metal iodide (MI$_2$ powder: PbI$_2$, Alfa Aesar, 99.999%; SnI$_2$, APL Engineered Materials, 99.999%) was evaporated and deposited onto quartz or glass

substrates at room temperature, achieving a pressure of approximately 1.0×10^{-6} Torr during the deposition. The powder was charged into a quartz crucible, and put into the chamber, and maintain the base pressure of about 4.0×10^{-7} Torr before starting the evaporation. The deposition rate (60-70 Å/min) and film thickness was monitored using a quartz crystal balance during the deposition. After deposition, the MI_2 films were quickly transferred into a nitrogen-filled drybox. The resultant films were transparent, with the SnI_2 film having a light greenish-yellow color and with the PbI_2 film yellow color. The thin films were homogeneous and smooth [59].

To Prepareorganic salt solutions, the organic ammonium iodides solutions were prepared by dissolving 107 mg of butylammonium iodide or 268 mg of phenethylammonium iodide in 1 mL of 2-propanol 6 mL of toluene was added to make the 2-propanol solution diluted. The molar concentrations for the phenethylammonium iodide solutions and the butylammonium iodide were 77 and 38 mM, respectively. Because of the limited solubility in the above mixed solvent, 7 mL of pure 2-propanol was utilized to dissolve 140 mg of methylammonium iodide to prepare a 127 mM solution of this organic salt. A solution of 2 equiv of butylammonium iodide and 1 equiv of methylammonium iodide was prepared by completely dissolving 80 mg of butylammonium iodide (0.40 mmol) and 32 mg of methylammonium iodide (0.20 mmol) in 5 mL of 2-propanol and then making it dilute with 25 mL of toluene. All the solutions were preserved in a nitrogen-filled drybox. The above mentioned butylammonium iodide solution was prepared by bubbling hydrogen iodide (Matheson Gas Products) into a butylamine (Aldrich) chloroform solution. Previously, phenethylammonium iodide and methylammonium iodide were synthesized by mixing aqueous solutions of the organic amine and hydriodic acid and drying the product under vacuum.

Finally, prepared each MI_2 thin film was dipped into a solution of the desired organic ammonium iodide in iso-propanol for a selected period of time in a nitrogen-filled drybox. After that it was quickly immersed in a rinse solution, which had the same composition as the dipping solution solvent (without the dissolved organic ammonium salt) for 5-10 s, to remove any excess organic ammonium salt. Before the film was taken out of the drybox for measurements, it was pumped in the drybox loading lock for 10 min to make sure that any remaining solvent was removed.

The sequential methods are much better control process over the perovskite morphology than the chemical method by allowing better PbI_2 confinement into the nanoporous network of TiO_2. By using this technique, 15% PCE was achieved [73, 75,76].

5.4 Vapour-Assisted Solution Method

Chen et al. presented a novel low-temperature approach for the deposition of a perovskite layer [77]. In this typical process, lead iodide films were deposited onto FTO glass which was coated by a compact layer of TiO_2. To form the perovskite films, lead iodide/TiO_2/FTO/glass stacks were annealed in an ambient of organic ammonium iodide vapour and N_2 at 150 °C for 2 hrs. It exhibited full surface coverage, uniform grain structure with grain size up to micrometers, and 100% precursor transformation. This excellent perovskite film in solar cells demonstrated 12.1% efficiency.

6. Summary and future prospects

Perovskite materials show tremendous progress in the advancements of perovskite solar cells within a few years. It brings enormous hopes and receives special scientific attention to scientific community. It already has achieved more than 15% efficiency in this field. On-going efficiency improvements and optimal cell designs with rapidly growing understanding of their material properties are expected.

Perovskite solar cells have several advantages over the existing photovoltaic technologies include material properties and fabrication process that could be simplifies the manufacture of high-performance devices. The diversity in proven methods may give rise

to low processing costs and simple application of attractive products, such as transparent, flexible or all-perovskite tandem cell modules. Moreover, this diversity may also allow perovskite cells to be directly integrated with other cell technologies to form high-performance tandem cells; Si and CIGS modules appear particularly promising in this aspect [78, 79].

The toxicity of Pb in perovskite solar cell is a concern, but not a major impediment to large-scale production and/or professional applications, the CdTe solar cell already proved that by gaining a reasonable market share. The danger is that technology dependent on toxic materials may be increasingly marginalized as legislation becomes increasingly more universal and restrictive. In that case, exclusion of Pb seems the only perfect solution. Significant PCE already achieved by replacing Pb by Sn [80, 81]. Alternatively, research into the present perovskites might allow more precise purpose of the features that have resulted in such rapid progress with encouraging identification and investigation of non-toxic material systems with similar properties.

Perovskites have the advantage that they provide multiple paths to commercialization. To compete the commercially established crystalline Si solar cells, extensive research is needed by developing new perovskite materials. There is an opportunity to develop high-performance tandem cell technology that uses both perovskite and existing technologies; this may allow introducing a new premium product in a commercial market. Additionally, effective measures should be taken on drawbacks, stability and industrialization of perovskite hybrid solar cells.

Acknowledgements

References

[1] Bisquert, J. Photovoltaics: the two sides of solar energy. Nature Photon. **2**, 648 (2008).

[2] M. A. Green, K. Emery, Y. Hishikawa, W. Warta, E. D. Dunlop. Progress in Photovoltaics Research and Application, **21**, 827 (2013).

[3] S. Kazim, Md. K. Nazeeruddin, M. Grätzel. Angewandte Chemie International edition 2014, doi: 10.1002/anie.201308719.

[4] Y. Tachibana, H. Y. Akiyama, Y. Ohtsuka. Chemistry Letters, **36**, 88 (2007).

[5] I. Robel, V. Subramanian, M. Kuno, P. V. Kamat, Journal of the American Chemical Society, **128**, 2385 (2006).

[6] O. Niitsoo, S. K. Sarkar, C. Pejoux, S. Rühle, D. Cahen, G. Hodes. Journal of Photochemistry and Photobiology A: Chemistry, **181**, 306 (2006).

[7] L. J. Diguna, Q. Shen, J. Kobayashi, T. Toyoda, Applied Physics Letters, **91**, 23116 (2007).

[8] R. Plass, S. Pelet, J. Krueger, M. Grätzel, U. Bach, The Journal of Physical Chemistry B **106**, 7578 (2002)

[9] P. Hoyer, R. Könenkamp. Applied Physics Letters, **66**, 349 (1995).

[10] A. Zaban, O. I. Mićić, B. A. Gregg, A. J. Nozik, Langmuir, **14**, 31533156 (1998).

[11] P. Yu, K. Zhu, A. G. Norman, The Journal of Physical Chemistry B, **110**, 25451 (2006).

[12] B. O'Regan, M. Grätzel, Nature, **353**, 737 (1991)

[13] A. Yella, H. N. Lee, C. Tsao, Science, **334**, 629 (2011).

[14] E. H. Sargent, Nature Photonics, **6**, 133 (2012).

[15] A. H. Ip, S. M. Thon, S. Hoogland, O. Voznyy, D. Zhitomirsky, R. Debnath, L. Levina, L. R. Rollny, G. H. Carey, A. Fischer, K. W. Kemp, I. J. Kramer, Z. Ning, A. J. Labelle, K. W. Chou, A. Amassia, E. H. Sargent, Nature Nanotechnology, **7**, 577 (2012)

[16] J. Tang, K. Kemp, S. Hoogland. Nature Materials, **10**, 765 (2011).

[17] R. Zhu, C. Y. Jiang, B. Liu, Advanced Materials, **21**, 994 (2009).

[18] G. Li, R. Zhu, Y. Yang, Nature Photonics, **6**, 153 (2012).

[19] M. Wang, C. Grätzel, S. M. Zakeeruddin, M. Grätzel. Energy Environmental Science **5**, 9394 (2012).

[20] H.. N. Tsao, C. Yi, T. Moehl, J. H. Yum, S. M. Zakeerudin, M. K. Nazeeruddin, M. Grätzel, Chemistry and sustainability energy and materials **4**, 591 (2011).

[21] S. M. Zakeerudin, M. Grätzel, Advanced Functional Materials, **19**, 2187 (2009)

[22] M. Gorlov, L. Kloo, Dalton Trans 2008, 2655.

[23]. H. Y. Chen, D. B. Kuang, C. Y. J. Su, Journal of Materials Chemistry, **22**, 15475 (2012)

[24] M. Yu, Y. Z. Long, B. Sun, Z. Fan, Nanoscale, **4**, 2783 (2012).

[25] Y. S. Yen, H. H. Chou, Y. C. Chen, C. Y. Hsu, J. T. Lin, Journal of Materials Chemistry, **22**, 8734 (2012).

[26] J. H. Noh, S. H. Im, J. H. Heo, T. N. Mandal, S. II. Seok. Nano Letters, **13**, 1764 (2013)

[27] H. S. Kim, C. R. Lee, J. H. Im, K. B. Lee, T. Moehl, A. Marchioro, S. J. Moon, R. Humphry-Baker, J. H. Yum, J. E. Moser, M. Grätzel, N. J. Park, Science Reports, **2**, 591 (2012)

[28] M. M. Lee, J. Teuscher, T. Miyasaka, T. N. Murakami, S. J. Snaith. Science, **338**, 643 (2012)

[29] A. Kojima, K. Teshima, Y. Shirai, T. Miyasaka, Journal of the American Chemical Society **131**, 6050 (2009).

[30] I. Koutselas, P. Bampoulis, E. Maratou, T. Evagelinou, G. Pagona, G. C. Papavassiliou, The Journal of Physical Chemistry C, **115**, 8475 (2011).

[31] C. R. Li, H. T. Deng, J. Wang, Y. Y. Zheng, W. J. Dong. Materials Letters, **64**, 2735 (2010)

[32] G. S. Patrin, N. V. Volkov, I. V. Prokhorova, Physics of the Solid State, **46**, 1891 (2004).

[33] Z. Cheng, J. Lin, CrystEngComm, **12**, 2646 (2010).

[34] I. Chung, B. Lee, J. He, R. P. H. Chang, M. G. Kanatzidis, Nature, **485**, 486 (2012).

[35] L. Etgar, P. Gao, Z. Xue, Q. Peng, A. K. Chandiran, B. Liu, M. K. Nazeeruddin, M. Grätzel, Journal of the American Chemical Society **134**, 17396 (2012).

[36] J. H. Im, C. R. Lee, J. W. Lee, S. W. Park, N. G. Park, Nanoscale, **3**, 4088 (2011).

[37] J. M. Ball, M. M. Lee, H. J. Snaith, Energy Environmental Science, **6**, 1739 (2013).

[38] N. -G Park, Journal of the Physical Chemistry Letters, **4**, 2423 (2013).

[39] Wenk, Hans-Rudolf; Bulakh, Andrei (2004). Minerals: Their Constitution and Origin. New York, NY: Cambridge University Press.

[40] A. Navrotsky, Chemistry Materials , **10**, 2787 (1998).

[41] V.M. Goldschmidt, Ber. Dtsch. Chem. Ges. **60,** 1263 (1927).

[42] M. Rini, et al. Nature **449,** 72 (2007).

[43] C. Li, et al. Acta Crystallogr. B **64**, 702 (2008).

[44] R.D. Shannon, Acta Crystallogr. A **32**, 751 (1976).

[45] Nam-Gyu Park, Perovskite solar cells: an emerging photovoltaic technology, Materials Today Volume 18, Number 2 _ March 2015.

[46] Martin A. Green, Anita Ho-Baillie & Henry J. Snaith, The emergence of perovskite solar cells, Nature Photonics **8**, 506 (2014).

[47] H. S. Kim, J. W. Lee, N. Yantara, P. P. Boix, S. A. Kulkarni, S. Mhaisalkar, M. Grätzel, N. G. Park, Nano Letters **13**, 2412 (2013).

[48] W. A. Laban, L. Etgar, Energy & Environmental Science, **6**, 3249 (2013)

[49] D. Liu, T. L. Kelly. Nature Photonics 2013, doi: 10.1038/nphoton.2013.342.

[50] G. E. Eperson, S. D. Stranks, C. Menelaou, M. B. Johnston, L. Herz, H. Snaith, Energy & Environmental Science, **7**, 982 (2014).

[51] P. P. Boix, K. Nonomura, N. Mathews, S. Mhaisalkar, Materials Today, **17**, 16 (2014).

[52] T. Baikie, Y. Fang, J. M. Kadro, M. Schreyer, F. Wei, S. G. Mhaisalkar, M. Grätzel, T. J. White, Journal of Materials Chemistry A, **1**, 5628 (2013).

[53] J. Qiu, Y. Qie, K. Yan, M. Zhong, C. Mu, H. Yan, S. Yang. Nanoscale, **5**, 3245 (2013).

[54] K. Tvrdy, P. A. Frantsuzov, P. V. Kamat, Proceedings of the National Academy of Science. U. S. A., **108**, 29 (2010).

[55] I. Robel, M. Kuno, P. Kamat, Journal of the American Chemical Society, **129**, 4136 (2007)

[56] J. H. Noh, N. J. Jeon, Y. C. Choi, M. K. Nazeeruddin, M. Grätzel, S. I. Seok, Journal of

Materials Chemistry A, **1**, 11842 (2013).

[57] G. E Eperson, V. M. Burlakov, P. Docampo, A. Goriely, H. J. Snaith. Advanced Functional Materials, **24**, 151 (2014).

[58] E. Edri, S. Kirmayer, D. Cahen, G. Hodes, The Journal of Physical Chemistry Letters **4**, 897 (2013)

[59] M. Liu, M. B. Johnston, H. J. Snaith, Nature, **501**, 395 (2013).

[60] M. H. Kumar, N. Yantara, S. Dharani, M. Grätzel. S. M. Mhaisalkar, P. P. Boix, N. Mathews, Chemical Communications, **49**, 11089 (2013).

[61] D. Bi, S. J. Moon, L. Haggman, G. Boschloo, L. Yang, E. M. J. Johansson, M. K. Nazeeruddin, M. Grätzel, A. Hagfeldt, RSC Advances, **3**, 18762 (2013).

[62] J. H. Heo, S. H. Im, J. H. Noh, T. N. Mandal, C. S. Lim, J. A. Chang, Y. H. Lee, H. J. Kim, A. Sarkar, M. K. Nazeeruddin, M. Grätzel, S. II. Seok, Nature Photonics, **7**, 486 (2013)

[63] G. Niu, W. Li, F. Meng, L. Wang, H. Dong, Y. Qiu, Journal of Materials Chemistry A **2**, 705 (2014)

[64] Research Cell Efficiency Records, NREL. http://www.nrel.gov/ncpv/.

[65] Severin N. Habisreutinger, Tomas Leijtens, Giles E. Eperon, Samuel D. Stranks, Robin J. Nicholas, and Henry J. Snaith, Carbon Nanotube/Polymer Composites as a Highly Stable Hole Collection Layer in Perovskite Solar Cells, Nano Lett., , **14**(10), 5561 (2014).

[66] Sun, S. et al. Energy Environ. Sci. **7**, 399 (2014).

[67] Wehrenfennig, C., Liu, M., Snaith, H. J., Johnston, M. B. & Herz, L. M. Homogeneous emission line broadening in the organo lead halide perovskite $CH_3NH_3PbI_3-xCl_x$. J. Phys. Chem. Lett. **5**, 1300 (2014).

[68] C. C. Stoumpos, C. D. Malliakas, M. G. Kanatzidis, Inorganic Chemistry, **52**, 9019 (2013).

[69] N. Kitazawa, Y. Watanabe, Y. Nakamura, Journal of Materials Science, **37**, 3585 (2002)

[70] K. Wojciechowski, M. Saliba, T. Leijtens, A. Abate, A. J. Snaith, Energy & Environmental Science, **7**, 1142 (2014)

[71] A. M. Salau, Solar Energy Materials, **2**, 327 (1980)

[72] D. B. Mitzi, Chemistry of Materials, **8**, 791 (1996).

[73] K. Liang, D. B. Mitzi, M. T. Prikas, Chemistry of Materials, **10**, 403 (1998).

[74] D. B. Mitzi, C. D. Dimitrakopoulos, L. L. Kosbar, Chemistry of Materials, **13**, 3283 (2001)

[75] J. Shi, J. Dong, S. Lv, Y. Xu, L. Zhu, J. Xiao, X. Xu, H. Wu, D. Li, Y. Luo, Q. Menga Applied Physics Letters:**104**, 063901 (2014).

[76] P. Gao, M. Grätzel, M. K. Nazeeruddin, Energy & Environmental Science 2014, doi:10.1039/c4ee00942h.

[77] Q. Chen, The Journal of American Chemical Society, **136**, 622 (2014).

[78] Snaith, H. J. Perovskites: the emergence of a new era for low-cost, high-efficiency solar cells. J. Phys. Chem. Lett. **4,** 3623 (2013).

[79] Service, R. F. Perovskite solar cells keep on surging. Science **344**, 458 (2014).

[80] Noel, N. K. et al. Lead-free organic-inorganic tin halide perovskites for photovoltaic applications. Energy Environ. Sci. http://dx.doi.org/10.1039/c4ee01076K (2014).

[81] Feng Hao1, Constantinos C. Stoumpos1, Duyen Hanh Cao1, Robert P. H. Chang2 and Mercouri G. Kanatzidis, Lead-free solid-state organic–inorganic halide perovskite solar cells, Nature Photonics, Volume: 8, Pages: 489–494 Year published: (2014).